Friction stir welded lap joint inspection using ultrasonic guided waves

Cite as: AIP Conference Proceedings **2102**, 050004 (2019); https://doi.org/10.1063/1.5099770
Published Online: 08 May 2019

Pierre Belanger, and Mohammad Jahazi

Friction Stir Welded Lap Joint Inspection Using Ultrasonic Guided Waves

Pierre Belanger[1,a)] and Mohammad Jahazi[1]

[1]Département de génie mécanique, École de technologie supérieure, 1100, rue Notre-Dame Ouest, Montréal, Québec, H3C 1K3, Canada

[a)] Corresponding author: pierre.belanger@etsmtl.ca

Abstract. Friction stir welding is a solid state joining process used across a range of industries from shipbuilding to aerospace. However, defects such as kissing bonds or wormholes usually associated with poor control of the rotational and traverse speeds during manufacturing remain difficult to detect using standard nondestructive testing methods. This paper investigates the correlation between the transmission of low-frequency ultrasonic guided waves through a lap joint and the rotational speed used during manufacturing. The aim of the method is therefore to nondestructively assess the manufacturing parameters rather than detect specific defects. The experimental setup comprises a 100 kHz shear transducer used for the excitation of S_0, six pairs of 3.2 mm aluminium plates in a friction stir welded lap joint configuration and a 2D laser Doppler vibrometer. The lap joints were manufactured with a rotational speed varying from 600 RPM to 1050 RPM while the traverse speed and the plunge were maintained constant. The experimental results showed excellent correlation between the transmission S_0 and the stir zone width. Clear outliers were also identified when looking at the amplitude of the 2nd harmonic of the S_0 mode.

INTRODUCTION

Friction stir welding (FSW) is still considered an emerging joining method although it was first published approximately 20 years ago [1]. It is used today in a range of industries including automotive, aerospace and naval. In FSW, a rotating tool is inserted at a joint interface and then travels along the joint interface. FSW can be used in lap, butt or T joint configurations over great length. FSW is known to have good repeatability and roughly constant properties along the weld line when the welding parameters are well controlled. However, a range of surface and sub-surface defects are associated with FSW. Surface defects such as scalloping, ribbon flash or surface galling can typically be detected through careful visual inspection. However, the sub-surface defects associated with FSW are notoriously difficult to detect [2]. Defects such as wormhole, nugget collapse or kissing bonds at the joint faying interface are hardly detected with standard NDT methods.

This project is therefore interested in comparing linear and nonlinear ultrasonic guided wave transmission through lap joints in a view to develop a method for joint quality screening. Linear transmission of ultrasonic guided waves is sensitive to changes in the cross-section of the waveguide or changes in the acoustic impedance [3]. On the other hand, the generation of nonlinear ultrasonic guided waves is typically associated with small changes in the material microstructure [4]. Therefore a combination of both methods could lead to a method able to accurately screen FSW joints as well as identify the potential causes of the defects. However, as both methods will be employed in the low-frequency regime defect, imaging or individual defect detection will not be possible. This paper begins with a description of the materials and methods followed by a section on results inside which the discussion is embedded.

MATERIALS AND METHODS

Ultrasonic guided waves propagate in elongated structures and are today regularly used to screen pipelines for defects. Below the cut-off frequency of the first high order mode, three fundamental modes can propagate as shown in figure 1: (1) A_0, (2) S_0 and (3) SH_0. However, only S_0 at very low frequency was shown to respect all the conditions for the generation of the 2nd order harmonic required in nonlinear analysis [5]. As this project is interested in comparing linear and nonlinear results S_0 was selected. When using S_0 in the nondispersive frequency range, it becomes possible to perform a linear and a nonlinear analysis using a single measurement with the appropriate equipment.

45th Annual Review of Progress in Quantitative Nondestructive Evaluation, Volume 38
AIP Conf. Proc. 2102, 050004-1–050004-8; https://doi.org/10.1063/1.5099770
Published by AIP Publishing. 978-0-7354-1832-5/$30.00

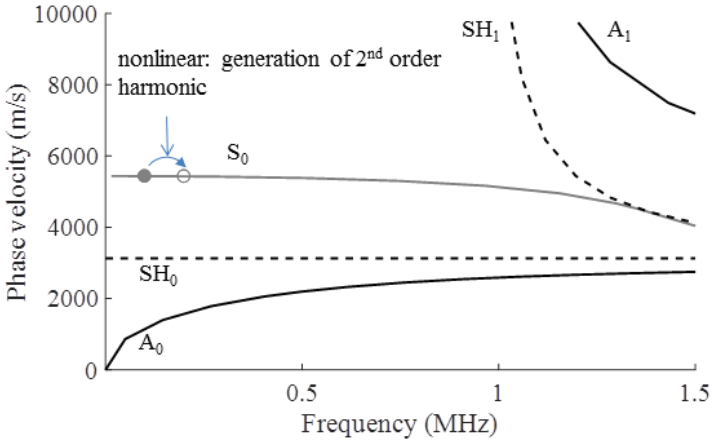

FIGURE 1. Phase velocity dispersion curve in a 3.2 mm aluminium plate.

In this project, 2024-T3 aluminium plates of 3.2 mm were welded in a lap joint configuration. A total of 6 sample joints were manufactured with dimensions shown in figure 2 (a). For all samples the travel speed was fixed to 1 mm/s. However, the tool RPM varied from 600 RPM to 1050 RPM in the following way: 2 samples at 600 RPM, 2 samples at 750 RPM, 1 sample at 900 RPM and 1 sample at 1050 RPM. The Friction Stirlink D-204 was used to manufacture all samples. Photos of the setup used for the manufacturing are shown in figure 2 (b) and (c).

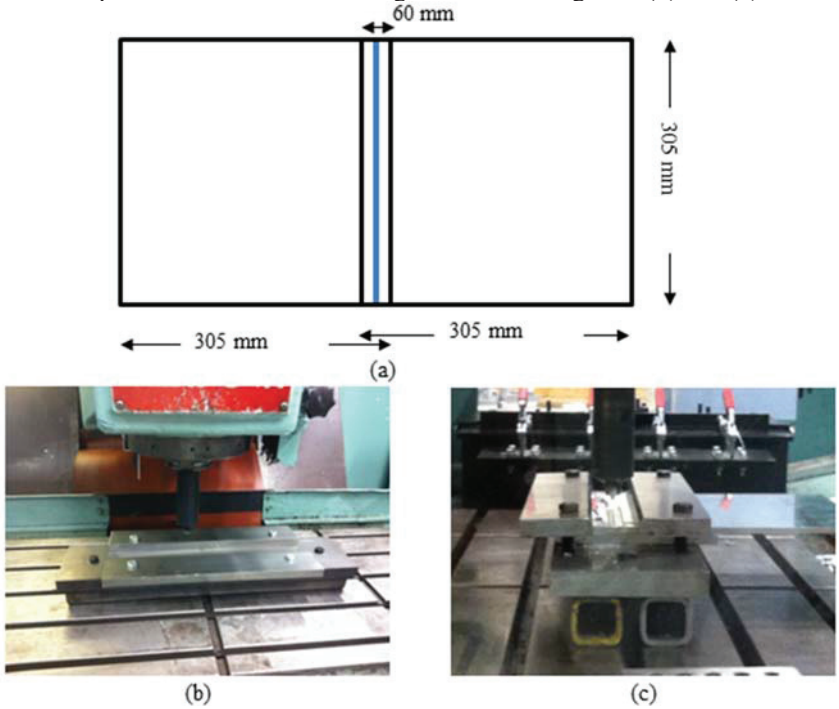

FIGURE 2. The dimensions of the FSW lap joint samples are shown in (a). (b) and (c) shows photos of the setup used in the manufacturing of the samples.

After manufacturing the 6 samples, cross-sections of each sample at the FSW joint were analyzed under the microscope to measure the width of the stir and the thermo-mechanically affected zones as well as the hook heights on the retreating and advancing sides. Figure 3 shows (a) a schematic of the weld cross-section and (b) and (c) examples of the cross-sections obtained at 750 RPM and 1050 RPM respectively obtained using a microscope. The cross-sectional parameters will be compared with the ultrasonic guided wave measurements in the results section.

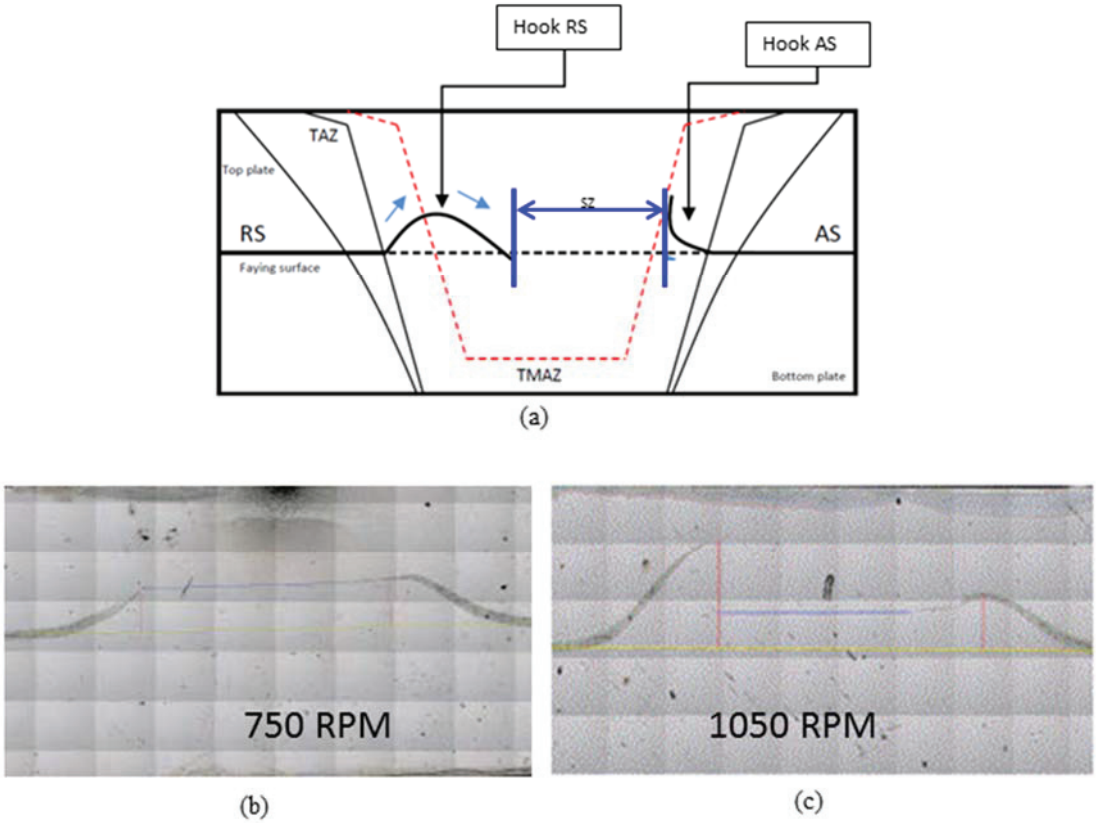

FIGURE 3. FSW cross-sectional analysis. (a) A schematic of the cross-section of FSW joints. RS and AS respectively stands for retreating and advancing side, SZ is the stir zone width and TMAZ is the thermos-mechanically affected zone. (b) and (c) respectively shows the cross-sections obtained at 750 RPM and 1050 RPM.

The ultrasonic guided wave measurements were conducted in the laboratory using a 100 kHz Olympus V1548 surface shear transducer. The transducer diameter was 25.4 mm. A shear transducer was used to maximize the excitation of the S_0 mode relative to the A_0 mode. Shear couplant and a clamp were used to ensure transmission of the excitation to the plate. For all measurements the transducer was mounted on the advancing side. The detection of the travelling ultrasonic guided waves was carried out using a dual laser Doppler vibrometer (Polytec OFV-505). A normal laser was combined with a second laser at 30° so as to separate the out-of-plane and in-plane displacement fields. Reflective tape was used to improve the signal received by the lasers. During the measurement, the test sample was mounted on a scanning table so as to move the laser detection point. A damping paste was used on the perimeter of the retreating side so as to reduce the amplitude of the waves reflected from the boundaries. A schematic and a photo of the experimental are presented in figure 4.

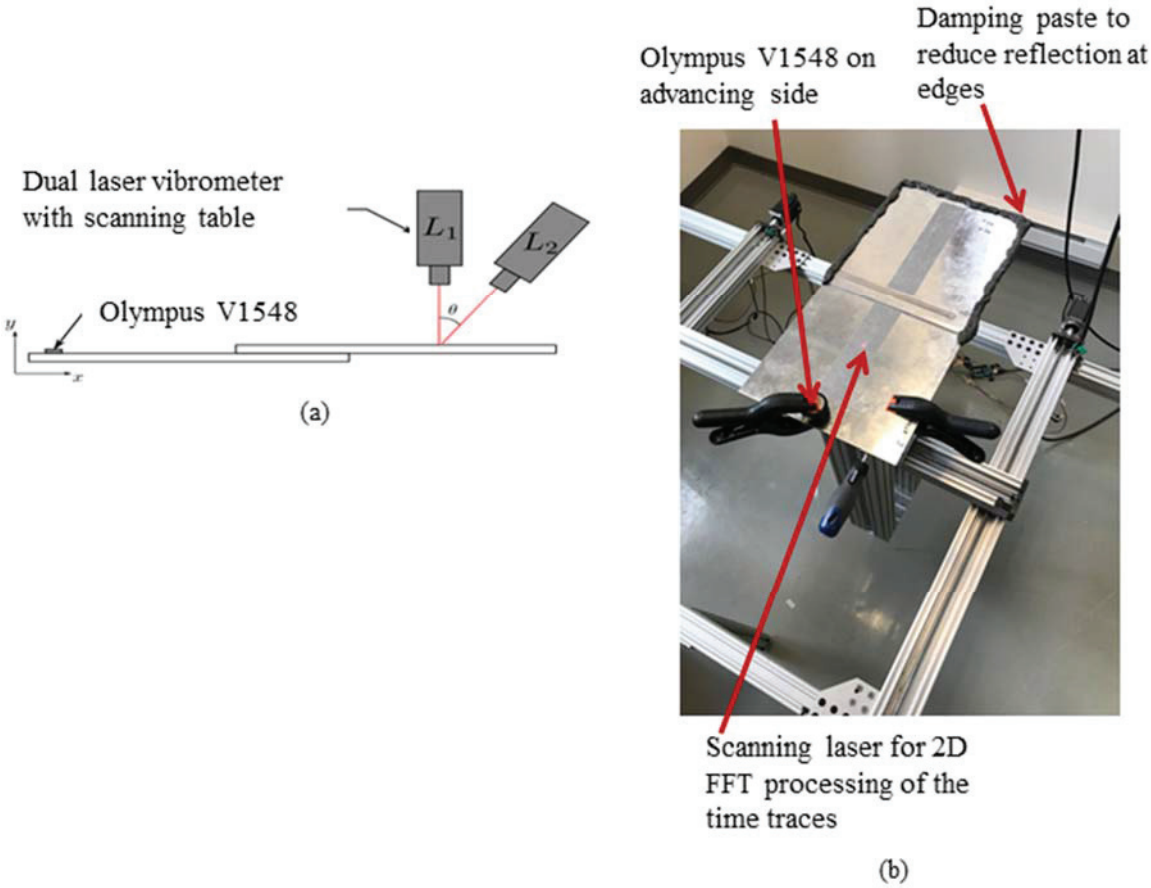

FIGURE 4. (a) schematic of the experimental setup and (b) a photo of the experimental setup.

As the dual laser system acquired out-of-plane and in-plane displacements at multiple points on the advancing and retreating sides, it was then possible to use the 2D FFT on the in-plane time traces to separate the received modes based on their wavenumbers and travelling direction. Figure 5 shows a typical 2D FFT map obtained from a finite element (FE) simulations using Pogo [6].

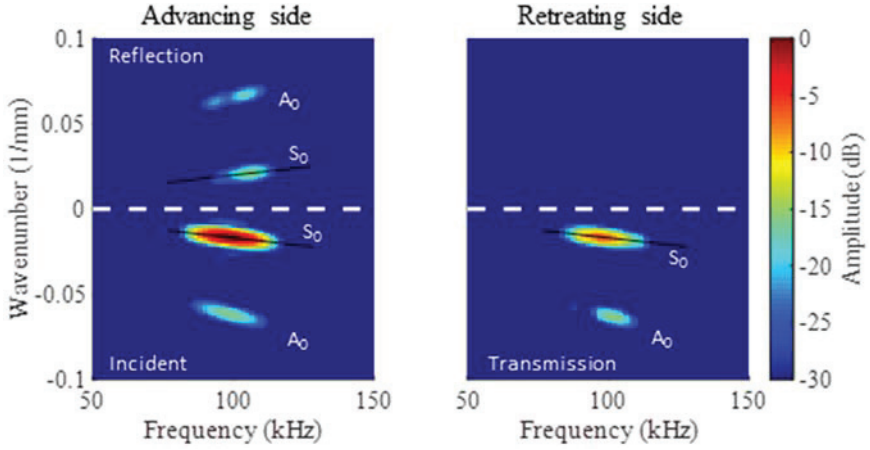

FIGURE 5: Example of an in-plane displacement 2D FFT obtained in a FE simulation.

As a shear transducer was used and only the in-plane displacement was considered in the 2D FFT, the incident wave ratio of amplitude between S_0 and A_0 was approximately 15 dB. The amplitude of the incident, reflected and transmitted S_0 was measured by averaging all the points at -6 dB around the maximum. Therefore, for the incident wave, the maximum amplitude of S_0 was detected and averaged with all the points -6 dB below its value. This

procedure was repeated for the reflected and transmitted modes. The reflection and transmission ratios were then calculated using the appropriate values.

For the nonlinear analysis, the signal processing had to be adapted. The signals were first bandpass filtered around 200 kHz. Instead of calculating ratios, the nonlinear parameter β was calculated for the incident, reflected and transmitted S_0:

$$\beta = \frac{A_2}{(A_1)^2} \tag{1}$$

where A_1 and A_2 are respectively the amplitude at the fundamental frequency and the amplitude at the 2nd harmonic. In this work, the fundamental frequency was 100 kHz and the 2nd harmonic was at 200 kHz. The incident β was considered as the baseline as it includes nonlinearities from the material but also from the measurement setup. Any significant changes in β in reflection or transmission would therefore be associated with the weld.

RESULTS AND DISCUSSIONS

The effect of the tool RPM on the cross-section properties are shown in figure 6.

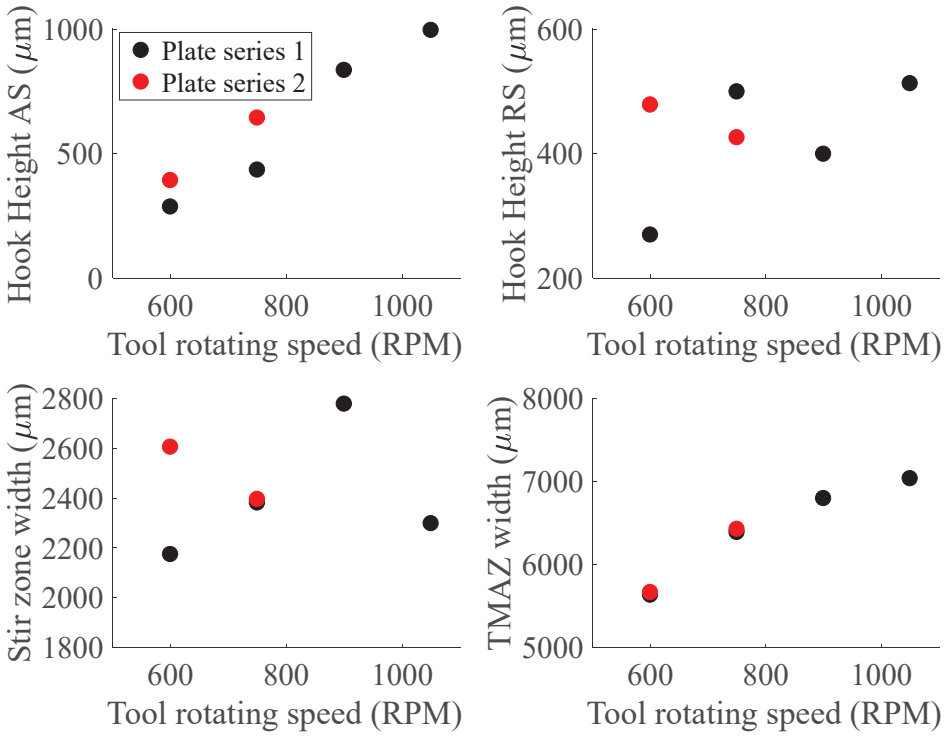

FIGURE 6. Variation of the cross-sectional properties as a function of the tool RPM.

The hook height on both sides appears to roughly increase as a function of the tool RPM. The width thermo-mechanically affected zone at the faying surface is clearly increasing with the tool RPM. Finally, width of the stir zone, which is often considered a very important parameter in FSW quality control doesn't appear to follow a clear trend. There is a maximum at 900 RPM with the second plate at 600 RPM not far below. It is also interesting to note that the two joints at 600 RPM are rather different in terms of the hook height on the retreating side and the stir zone width.

The ultrasonic guided wave measurements were repeated 3 times for each sample. Between each measurement, the transducer was removed from the plate and the plate was dismounted from the scanning table. Figure 7 shows a typical 2D FFT map obtained on the first sample at 600 RPM.

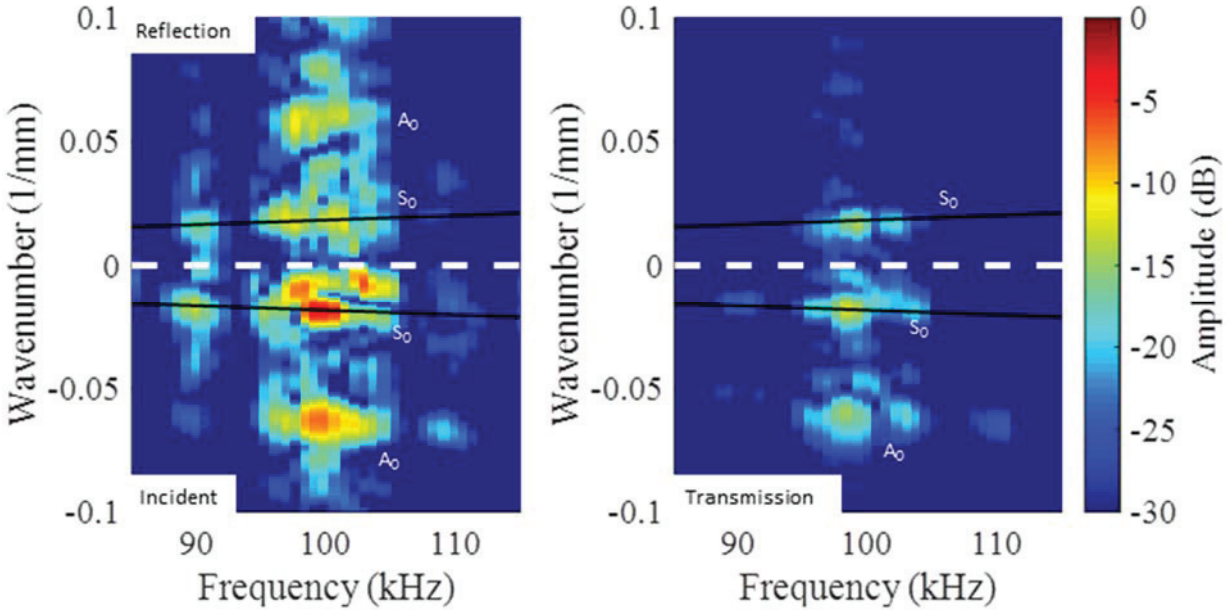

FIGURE 7. Typical 2D FFT obtained on the first sample at 600 RPM.

In figure 7, the A_0 and S_0 mode are identified and the black lines across both maps correspond to the S_0 dispersion curve. First thing to note is that the incident A_0 mode is much higher than in the simulation. This may become a source of error if a significant portion of this A_0 mode converts to S_0 when impinging the weld. Moreover, the damping paste appears to be highly efficient at suppressing the A_0 reflection from the plate edges but was unable to suppress the S_0 mode. Using the method described in the previous section, the reflection and transmission coefficient were measured: R = -6.9 dB and T = -10.2 dB. Figure 8 shows the reflection and transmission coefficient as a function of the tool RPM.

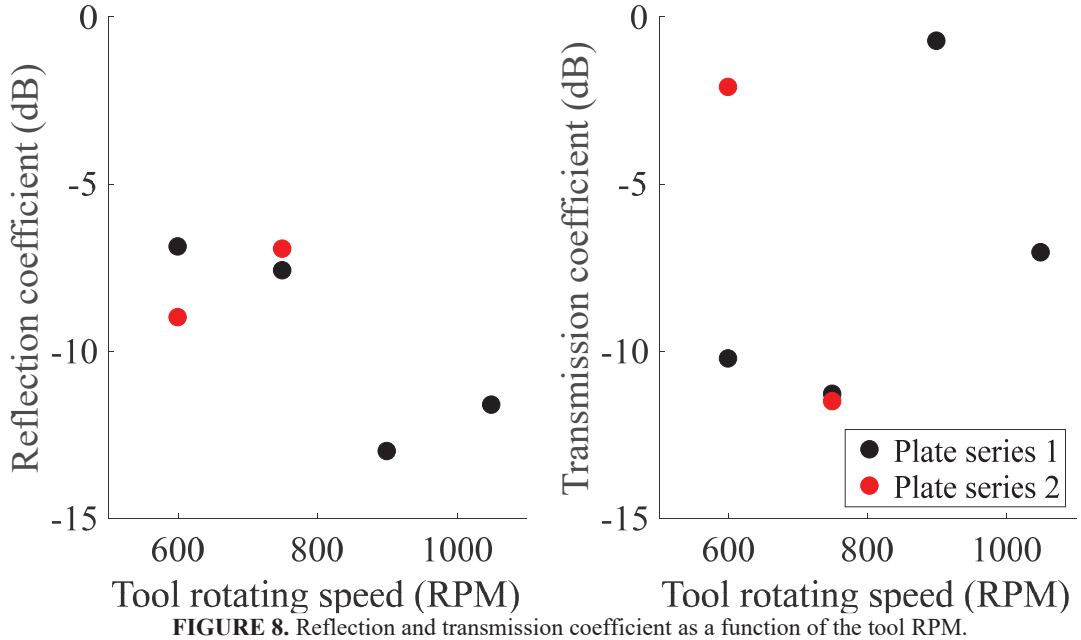

FIGURE 8. Reflection and transmission coefficient as a function of the tool RPM.

The evolution of the reflection and transmission coefficient as a function of the tool RPM is rather difficult to interpret. However, there are interesting points to note. The maximum transmission coefficient is obtained at 900 RPM followed by the second plate at 600 RPM in a similar way to what was observed for the stir zone width. Figure 9 therefore presents the transmission coefficient as well as the stir zone width as a function of the tool RPM.

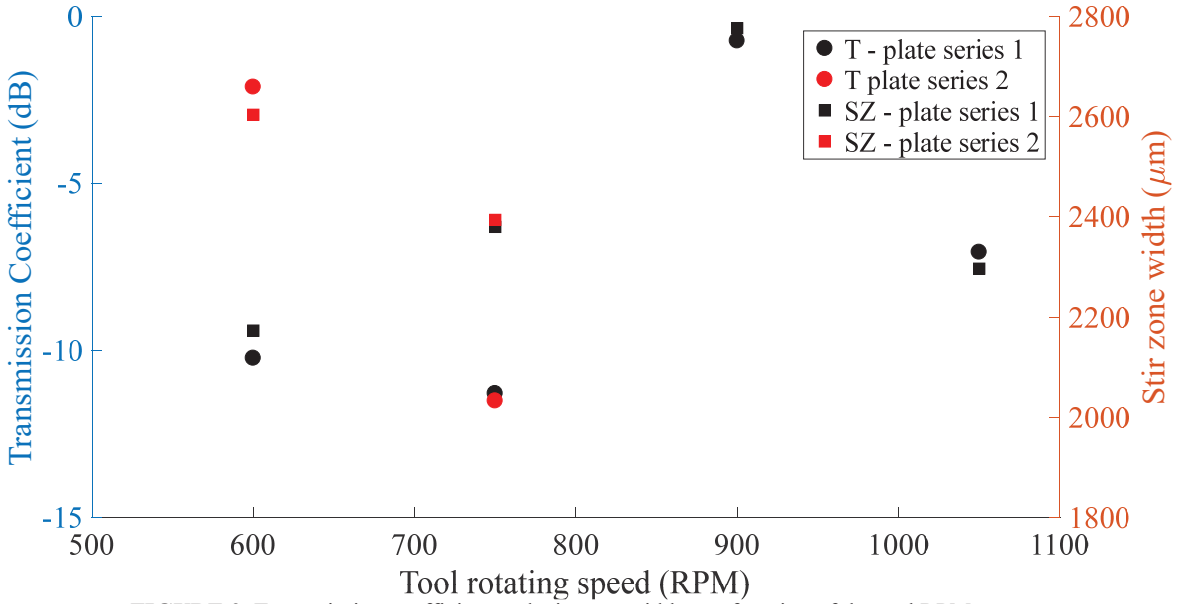

FIGURE 9. Transmission coefficient and stir zone width as a function of the tool RPM.

The correlation between the transmission coefficient and the stir zone width is remarkable. It appears that the transmission coefficient of the S_0 mode is directly correlated with the very important stir zone width. The transmission coefficient is even able to measure the difference between the two plates at 600 RPM. At 750 RPM the distance between the stir zone width and the transmission coefficient is the largest. However the measurements for the two plate series are repeatable. For reference, the stir zone width of all plates was always between 0.04 and 0.05 of the S_0 wavelength at 100 kHz.

The nonlinear measurements at the 2nd harmonic were also conducted and are presented in figure 10.

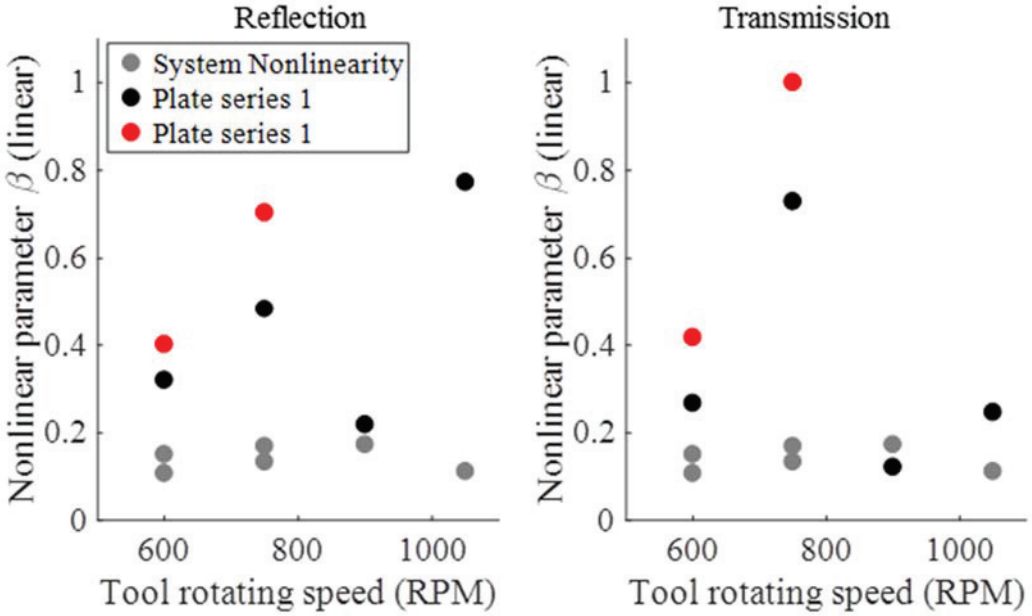

FIGURE 10. Evolution of nonlinear parameter β as a function of the tool RPM.

The system nonlinearity was evaluated on the incident wave for each measurement and appears to be always in the same range. In both reflection and transmission the plates welded at 750 RPM appear to be clear outlier with a β significantly above the system nonlinearity. However, no clear trend could be identified or correlated with the

microscopic measurement performed on the cross-sections. The interpretation of those results is a clear direction for future work.

CONCLUSION

Sub-surface defects associated with FSW lap joints are notoriously difficult to detect using standard NDT methods. This paper aimed at using low-frequency ultrasonic guided waves in a view to develop a quality screening method using both linear and nonlinear measurements. The correlation between the stir zone width and the S_0 transmission coefficient was striking. The transmission coefficient appears to be an excellent indicator of the stir zone width. When using the data at the 2nd harmonic of the S_0 mode, clear outliers were identified but not correlation was so far observed with cross-sectional images. Fatigue tests, shear punch tests as well as more detailed micrography are currently underway to help understand the nonlinear measurements.

ACKNOWLEDGMENTS

The work was supported by Quebec's aluminium research centre (REGAL). We also gratefully acknowledge the support of NVIDIA Corporation with the donation of the QUADRO P6000 GPU used for this research.

REFERENCES

1. W. Thomas and E. Nicholas, "Friction stir welding for the transportation industries", *Materials & Design* **18** (4-6), 269-273 (1997).
2. M. A. Fakih, S. Mustapha, J. Tarraf, G. Ayoub and R. Hamade, "Detection and assessment of flaws in friction stir welded joints using ultrasonic guided waves: experimental and finite element analysis", *Mechanical Systems and Signal Processing* **101**, 516-534 (2018).
3. A. Demma, P. Cawley, M. Lowe, A. Roosenbrand and B. Pavlakovic, "The reflection of guided waves from notches in pipes: a guide for interpreting corrosion measurements", *NDT & E International* **37** (3), 167-180 (2004).
4. C. Bermes, J.-Y. Kim, J. Qu and L. J. Jacobs, "Experimental chracterization of material nonlinearity using Lamb waves", *Applied Physics Letters* **90** (2), 021901 (2007).
5. P. Zuo, Y. Zhou and Z. Fan, "Numerical and experimental investigation of nonlinear ultrasonic Lamb waves at low frequency", *Applied Physics Letters* **109** (2), 021902 (2016).
6. P. Huthwaite, "Accelerated finite element elastodynamic simulations using the GPU", *Journal of Computational Physics* **257**, 687-707 (2014).